Hepatitis B virus X protein promotes hepatocellular carcinoma invasion and metastasis via upregulating thioredoxin interacting protein

ZHILIANG HE[1,2*], YOUJIA YU[1,3*], YUNHONG NONG[1,2], LINGYAO DU[1,2], CONG LIU[1,2], YONG CAO[1,3], LANG BAI[1,2] and HONG TANG[1,2]

[1]Center of Infectious Diseases, West China Hospital, Sichuan University; [2]Division of Infectious Diseases, State Key Laboratory of Biotherapy and Cancer Center, West China Hospital, Sichuan University and Collaborative Innovation Center for Biotherapy; [3]Department of Forensic Pathology, Medical School of Basic and Forensic Sciences, Sichuan University, Chengdu, Sichuan 610041, P.R. China

Received September 14, 2015; Accepted February 23, 2017

DOI: 10.3892/ol.2017.6296

Abstract. Hepatitis B virus X protein (HBx), a multifunctional protein encoded by the X gene of the hepatitis B virus (HBV) is involved in the metastasis of HBV-associated hepatocellular carcinoma (HCC) through various pathways, including upregulating intracellular reactive oxygen species (ROS). Thioredoxin interacting protein (TXNIP) is a key mediator of intracellular ROS, but its function in HBx-mediated metastasis of HBV-associated HCC is elusive. In the present study, HBV-associated HCC tissues with or without metastasis and HepG2 cells were used to study the function of TXNIP in HBx-mediated metastasis of HBV-associated HCC. Initially, the expression levels of TXNIP and HBx in HBV-associated HCC tissues were detected by immunohistochemistry and reverse transcription-quantitative polymerase chain reaction. The results revealed that high expression of TXNIP may be an independent risk factor for metastasis of HBV-associated HCC, and the mRNA levels of TXNIP and HBx were positively associated. Secondly, the association between HBx and TXNIP was investigated using a HBx expression stable cell line, in which HBx expression was induced and controlled by doxycycline. The results demonstrated that HBx may upregulate TXNIP expression in HepG2 cells. Thirdly, the effects of TXNIP and HBx on HepG2 cell migration and invasion were studied by scratch and Matrigel invasion assays, respectively. The results demonstrated that TXNIP overexpression enhanced HepG2 cell migration and invasion. In addition, ectopic expression of HBx promoted HepG2 cell migration and invasion, and this effect may be attenuated by knockdown of TXNIP expression, which indicated that TXNIP may be involved in the process. In summary, the present results demonstrated that TXNIP may be involved in HBx-mediated metastasis of HBV-associated HCC.

Correspondence to: Professor Hong Tang, Center of Infectious Diseases, West China Hospital, Sichuan University, 37 Guoxue Alley, Chengdu, Sichuan 610041, P.R. China
E-mail: htang6198@hotmail.com

*Contributed equally

Key words: hepatocellular carcinoma, hepatitis B virus X protein, metastasis, thioredoxin interacting protein

Introduction

Hepatocellular carcinoma (HCC) accounts for between 85-90% of primary liver cancers, which is the fifth most common cancer and the third leading cause of cancer-associated mortality worldwide (1). Hepatitis B virus (HBV) infection is an important factor for HCC occurrence (2). The association between HBV and HCC has been demonstrated by multiple epidemiological studies: High HBV prevalence may result in a high frequency of occurrence of HCC, and the risk of HCC in HBV carriers is significantly increased compared with that of non-carriers (3,4). The main reason for poor prognosis of HCC is invasion of the portal vein, leading to the formation of a tumor thrombus and intrahepatic spread, which results in a high intrahepatic metastatic rate and recurrence rate following surgery (5).

Hepatitis B virus X protein (HBx), an important regulatory protein, may enhance the transcription and replication of HBV (6) and regulate biological processes, including host gene transcription, cell cycle, apoptosis and oxidative stress (7,8). Previous studies have demonstrated that HBx is an important factor in the development of HBV-associated HCC (9-11). Thus far, mechanisms of HCC metastasis promotion by HBx include: Promotion of epithelial-mesenchymal transition (EMT) (12,13); degradation of the extracellular matrix (ECM) (14,15); reduction of cell-ECM interactions (16); alteration of the cellular morphology conductive to migration and motility (17,18); repression of miRNA-148a (19) or upregulation of miRNA-143 (20). HBx may also upregulate intracellular ROS levels (21,22), and ROS have been demonstrated to regulate the expression of EMT and metastasis-associated genes,

including E-cadherin, integrin and matrix metalloproteinases in HCC cells, which contribute to HCC metastasis (23,24).

Thioredoxin interacting protein (TXNIP), also known as vitamin D3 upregulated protein 1, is involved in a wide range of cellular processes, including proliferation, apoptosis, lipid and glucose metabolism and redox regulation (25). TXNIP may also be involved in the metastasis of a variety of tumors (26-29) and may act as a key mediator of intracellular ROS levels through the TXNIP/thioredoxin/ROS axis (25), which contributes to the progression of tumors. However, the function of TXNIP in the metastasis of HCC remains to be investigated, and it is unclear whether TXNIP serves a function in HBx-mediated metastasis of HCC.

In the present study, the expression levels of HBx and TXNIP were investigated in HBV-associated HCC tissues, and the association between their expression levels and the metastasis of HBV-associated HCC was analyzed. The function of TXNIP in HBx-induced migration and invasion of HepG2 cells was also investigated. It was revealed that TXNIP expression in HBV-associated HCC tissues may be an independent risk factor for metastasis, and HBx may mediate metastasis of HBV-associated HCC through upregulating TXNIP expression.

Materials and methods

Patients and tissue specimens. In the present study, 62 HBV-associated HCC tissue samples were collected between October 2010 and August 2012 from West China Hospital, Sichuan University (Chengdu, China). The age of the patients ranged from 26 to 76 years (median, 46 years). Of the 62 patients, 54 were male and 8 were female. All the patients were confirmed by pathological diagnosis of HCC and had not received irradiation or chemotherapy prior to surgical operation. The patients were divided into two groups as follows: A metastatic group with portal vein thrombus or peripheral metastasis, and a non-metastatic group without portal vein thrombus and peripheral metastasis. The present study was approved by the Ethics Committee of West China Hospital, Sichuan University. Informed consent was obtained from all the patients or their relatives prior to analysis.

Tissue microarray construction and immunohistochemical staining. All 62 samples were used to construct tissue microarrays. Paraffin sections of the tissue microarrays were deparaffinized in xylene and rehydrated in graded ethanol. Antigen retrieval was performed in boiled 0.01 M citrate buffer (pH 6.0) for 2 min. Endogenous peroxidase was blocked by 3% H_2O_2 in PBS for 30 min at 37˚C. Sections were then incubated with rabbit anti-TXNIP antibody (dilution, 1:400; cat. no. SAB2108250; Sigma-Aldrich, St. Louis, MO, USA) overnight at 4˚C. Subsequently, sections were visualized using the EnVision G|2 System/AP (cat. no. K535521-2; Agilent Technologies, Inc., Santa Clara, CA, USA) and counterstained with Hematoxylin Staining Solution (cat. no. C0107; Beyotime Institute of Biotechnology, Haimen, China) for 5 min at room temperature, according to the manufacturer's instructions. A total of five randomly selected optical microscopic fields at x400 magnification for each sample were evaluated by two pathologists who were blind to the clinical data according to the Axiotis score standard (30). The intensity and percentage of positive cells were used to evaluate each section. Intensity was scored as follows: 0) No detectable staining; 1) weak staining; 2) moderate staining; and 3) strong staining. The scores for the percentage of positive cells were as follows: 0) Rate of 0-25% scored; 1) rate of 26-50%; 2) rate of 51-75%; and 3) rate of >75%. The total score was calculated by multiplying the intensity and positivity scores.

Cell culture and transfection or infection. The human HCC HepG2 cell line was purchased from American Type Culture Collection (ATCC; Manassas, VA, USA) and cultured at 37˚C in a 5% CO_2 atmosphere, in Dulbecco's modified Eagle's medium (DMEM; Invitrogen; Thermo Fisher Scientific, Inc., Waltham, MA, USA) supplemented with 10% fetal bovine serum (FBS; Gibco; Thermo Fisher Scientific, Inc.). The HEK 293T cell line was purchased from ATCC and cultured at 37˚C in a 5% CO_2 atmosphere, in RPMI-1640 medium (Invitrogen; Thermo Fisher Scientific, Inc.) supplemented with 10% FBS. Cells were seeded onto 6-well plates 24 h before transfection or infection. Cells were transfected with purified plasmids constructed in the present study [pTRE-Tight-HBx, pEGFP-N1-TXNIP, pSicoR-TXNIP short hairpin (sh) RNA] or preserved in our lab (pBabe-puro, pEGFP-N1, pNKF, pNKF-HBx, pSicoR, psPAX2 and pMD2G) using X-tremeGENE HP DNA transfection reagent (Roche Diagnostics GmbH, Mannheim, Germany), according to the manufacturer's protocol, or infected with lentivirus constructed in the present study as previously described (31).

Construction of the HBx expression stable cell line. pNKF-HBx and pTRE-Tight plasmids from the Tet-On Advanced Inducible Gene Expression System (Clontech Laboratories, Inc., Mountain View, CA, USA) were digested with *Not* 1 and *Xba* 1 (Takara Bio, Inc., Otsu, Japan). The digested HBx gene with FLAG sequence was inserted into the digested pTRE-Tight plasmid. pTRE-Tight-HBx and pBabe-puro plasmid with puromycin resistant was preserved in our lab, they were then co-transfected into HepG2 Tet-On Advanced cells (Clontech Laboratories, Inc.) in the proportion of 10:1. Puromycin-resistant clones were treated with gradient concentrations (0.1-0.25 mg/l) of doxycycline (Dox; Sigma-Aldrich) and tested for HBx expression, as well as inducing efficiency, by western blot analysis as described below. Clones with low constitutive expression and high inducing efficiency were selected for subsequent investigation.

Overexpression of TXNIP in HepG2 cells. pEGFP-N1 was preserved in our lab. Total RNA was extracted with TRIzol® reagent (Invitrogen; Thermo Fisher Scientific, Inc.) from HepG2 cells and reverse transcribed into cDNA using PrimeScript RT Master mix (Takara Bio, Inc.), according to the manufacturer's protocol, and used as a template for TXNIP gene amplification by polymerase chain reaction (PCR) using PrimeSTAR HS DNA Polymerase (Takara Bio, Inc.). The cycling conditions for PCR were: 5 min incubation at 95˚C, followed by 30 cycles of 98˚C for 5 sec, 60˚C for 5 sec and 72˚C for 90 sec. The primer sequences used were as follows: TXNIP forward (F), 5'-GACGCGCTCGAGATGGTGATGTTCAAGAAG-3' and reverse (R), 5'-CACCTGGTCGACTGCTGCACATTGTT GTTG-3'. The PCR products were digested with *Xho* 1 and

Sal 1 (Takara Bio, Inc.) ligated into pEGFP-N1 (also digested with *Xho 1* and *Sal 1*). HepG2 cells were transfected with pEGFP-N1-TXNIP or pEGFP-N1 as a negative control. TXNIP expression was detected by western blot analysis as described below.

Knockdown of TXNIP in HepG2 cells. Lentivirus system pSicoR, pxPAX2 and pMD2.G were preserved in our lab. The oligonucleotides (5'-TGCCACACTTACCTTGCCAATGTC AAGAGCATTGGCAAGGTAAGTGTGGCTTTTTTC-'3and 5'-TCGAGAAAAAAGCCACACTTACCTTGCCAATGCTC TTGACATTGGCAAGGTAAGTGTGGCA-3') encoding shRNA targeting TXNIP were digested with *Hpa* 1 and *Xho* 1 (Takara Bio, Inc.) and ligated into pSicoR (also digested with *Hpa* and *Xho* 1) using the DNA Ligation kit Ver.2.1 (Takara Bio, Inc.) according to manufacturer's protocol. pSicoR-TXNIP shRNA or pSicoR, psPAX2 and pMD2 G were co-transfected into HEK 293T cells in the proportion of 4:3:1 as previously described (32), lentivirus-containing supernatant were harvested 48 h post transfection. HepG2 cells were infected with TXNIP shRNA lentivirus or pSicoR lentivirus. Knockdown efficiency of TXNIP was evaluated by western blot analysis.

Reverse transcription-quantitative PCR (RT-qPCR). For RT-qPCR, total RNA was extracted with TRIzol reagent (Invitrogen; Thermo Fisher Scientific, Inc.) from frozen HCC tissues and reverse transcribed into cDNA using PrimeScript RT Master Mix (Takara Bio, Inc.), according to the manufacturer's protocol. RT-qPCR was then performed using a Light Cycler 96 with Fast Start Universal SYBR-Green Master mix (Roche Diagnostics GmbH). The cycling conditions for PCR were: initial denaturation 95°C for 120 sec, then 40 cycles of 95°C at 10 sec, 62°C at 15 sec and 72°C at 30 sec. Glyceraldehyde 3-phosphate dehydrogenase (GAPDH) was used as the internal reference. Relative gene expression level was analyzed using the 2-ΔΔcq method (33). The primer sequences were as follows: TXNIP, F, 5'-CTCTGCTCGAATTGACAGAAAAGGATT-3' and R, 5'-CGCATGTCCCTGAGATAATATGATTGC-3'; HBx, F, 5'-GACTCCCCGTCTGTGCCTTCTCATC-3' and R, 5'-AGACCAATTTATGCCTACAGCCTCC-3'; GAPDH, F, 5'-AGGAGCGAGATCCCTCCAAAATCAAGT-3' and R, 5'-TGAGTCCTTCCACGATACCAAAGTTGT-3'.

Western blot analysis. For detection of Flag-HBx, HBx expression stable cells were cultured at 37˚C in a 5% CO_2 atmosphere, in DMEM supplemented with 10% FBS and gradient concentrations (0.1-0.25 mg/l) of Dox for 48 h. Proteasome inhibitor MG132 (10 μM, Sigma-Aldrich) was added to the medium 12 h prior to extracting total protein with SDS-PAGE loading buffer (Beyotime Institute of Biotechnology). For detection of TXNIP, cells were lysed in M_2 buffer (34). Equal amounts of protein extracts (60 μg) were separated by 12% SDS-PAGE and transferred to polyvinylidene fluoride membranes (Merck Millipore, Darmstadt, Germany). Membranes were then blocked at room temperature in 5% non-fat milk in Tris-buffered saline with 0.05% Tween-20 (TBS-T) for 1 h, followed by incubation with primary antibody against Flag-HBx (dilution, 1:1,000; cat. no. A2220; Sigma-Aldrich) or TXNIP antibody (dilution, 1:100; cat. no. sc-33099; Santa Cruz Biotechnology, Inc., Dallas, TX, USA) overnight at 4˚C. The membranes were then incubated with horseradish peroxidase-conjugated secondary antibody (dilution, 1:5,000; cat. no. ZDR-5307; ZSGB-BIO, Beijing, China) at room temperature for 1 h and visualized with enhanced chemiluminescence western blotting substrate (Pierce; Thermo Fisher Scientific, Inc.).

Scratch assay. HepG2 cells transfected and/or infected with pEGFP-N1, pEGFP-N1-TXNIP, pSicoR lentivirus, TXNIP shRNA lentivirus, pNKF, pNKF-HBx, pNKF-HBx in combination with TXNIP shRNA lentivirus were collected and seeded onto 12-well plates at a density of $3x10^6$ cells per well. Monolayer cultures were scratched with 200 μl tips. Serum-free DMEM medium was added and optical microscopic images of the scratches at 0 and 24 h were captured at x100 magnification. Each experimental group took three scratches, and each experiment repeated three times. Scratch space was analyzed with Image J software (version 1.41; National Institutes of Health, Bethesda, MD, USA). Relative cell migration distance (%) = 100 A - B)/A, where A is the width of the scratch at 0 h and B is the width of the scratch at 24 h (35).

Matrigel invasion assay. Matrigel invasion assays were performed using Transwell chambers (24-well insert; pore size, 8 μm; BD Biosciences, Franklin Lakes, NJ, USA). HepG2 cells transfected and/or infected with pEGFP-N1, pEGFP-N1-TXNIP, pSicoR lentivirus, TXNIP shRNA lentivirus, pNKF, pNKF-HBx, pNKF-HBx in combination with TXNIP shRNA lentivirus were collected in serum-free DMEM medium and seeded into the top chamber coated with Matrigel (BD Biosciences) at a density of $1x10^5$ cells per well. The lower chamber was filled with DMEM medium supplemented with 10% FBS. Following incubation for 24 h, the upper layer of Matrigel was removed. The cells on the underside of the filter were fixed by anhydrous methanol and stained with hematoxylin (Beyotime Institute of Biotechnology). Cell number was counted in five random optical microscopic fields at x200 magnification. Three chambers were used per experimental condition.

Statistical analysis. Data are presented as the mean ± standard deviation. Statistical analysis was performed using SPSS 20 software (IBM SPSS, Armonk, NY, USA). Receiver operating characteristic (ROC) curve analysis was applied to determine the cut-off score for TXNIP expression in HBV-associated HCC tissues as previously described (36). The independent sample Student's t-test was performed to analyze the variables between two groups. The χ^2 test was used to analyze the associations between TXNIP expression and clinicopathological features of patients with HBV-associated HCC. Univariate and multivariate logistics regression analysis was used to analyze the risk factors associated with metastasis of HBV-associated HCC. Spearman's rank correlation coefficient tests were used to assess the correlations between TXNIP and HBx in HBV-associated HCC tissues.

Results

TXNIP expression in HBV-associated HCC tissues and its association with clinicopathological features of patients

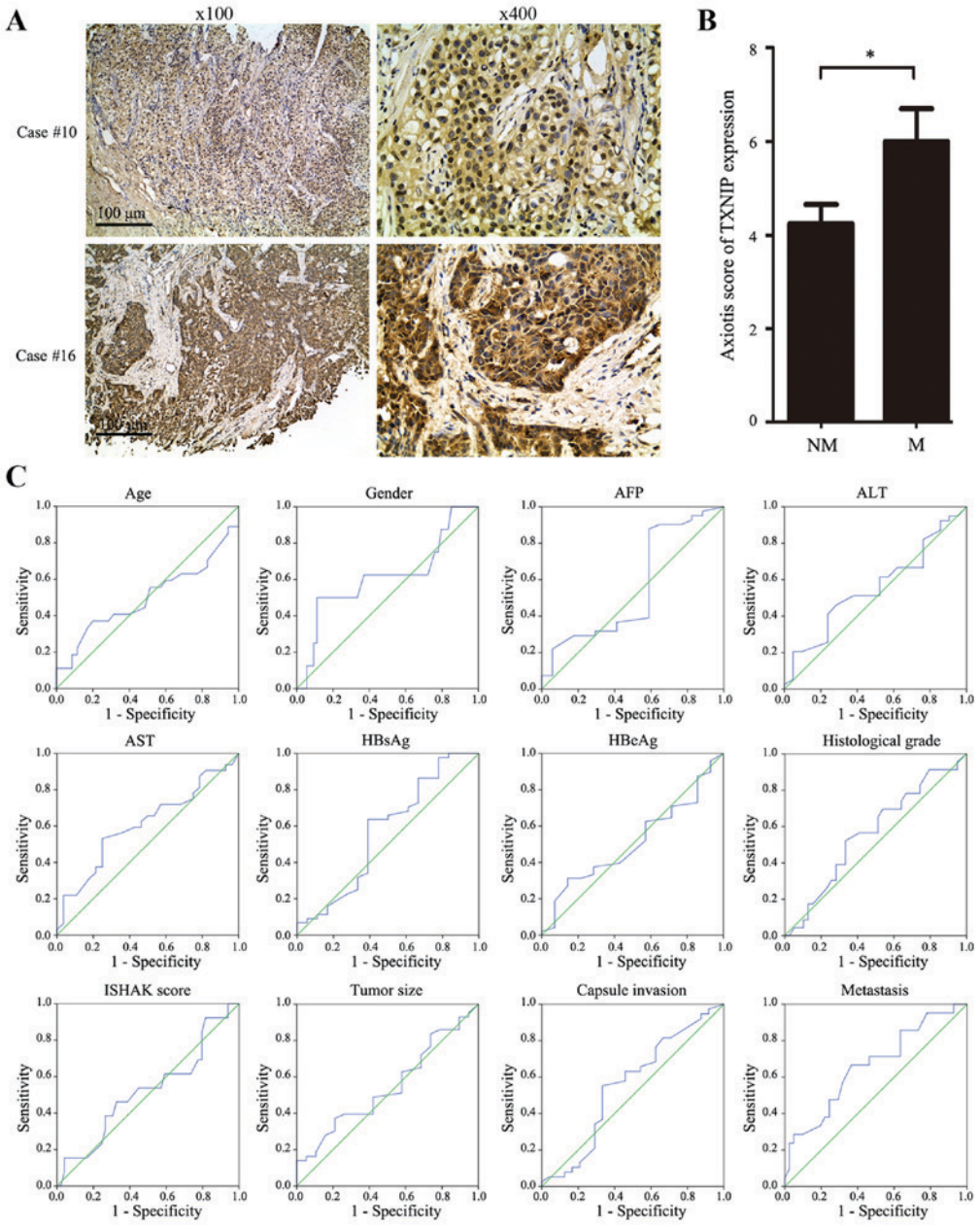

Figure 1. Expression levels of TXNIP in HBV-associated HCC tissues. (A) TXNIP expression in representative tissues. Case 10, tissue without metastasis; case 16, tissue with metastasis; scale bar, 100 μm. (B) Statistical analysis of TXNIP expression levels in NM and M HBV-associated HCC tissues. (C) The cut-off score for TXNIP expression was determined by receiver operating characteristic curve analysis. The sensitivity and specificity for each clinicopathological feature at different TXNIP scores were plotted. *P<0.05 vs. NM. TXNIP, thioredoxin interacting protein; HBV, hepatitis B virus; HCC, hepatocellular carcinoma; NM, non-metastatic; M, metastatic; AFP, α-fetoprotein; ALT, alanine transaminase; AST, aspartate transaminase; HBsAg, surface antigen of hepatitis B virus; HBeAg, hepatitis B viral protein.

with HBV-associated HCC. TXNIP expression of the tissue microarray was detected by immunohistochemical staining and evaluated according to the Axiotis score standard. TXNIP expression in representative samples of HBV-associated HCC tissues is depicted in Fig. 1A. The results of statistical analysis revealed that TXNIP scores of the metastatic group (6.000±3.185) increased compared with those of the non-metastatic group (4.244±2.634; P=0.024; Fig. 1B). According to the cut-off score determined by the ROC curve analysis (Fig. 1C), low expression of TXNIP in HCC tissues was defined when the TXNIP score was <4.9 and high expression was defined when the TXNIP score was ≥4.9. The χ^2 test demonstrated that TXNIP expression levels were positively associated with metastasis of HBV-associated HCC (Table I). Additional multivariate logistic regression analysis revealed that besides age, tumor size and histological grade, high expression of TXNIP in HCC tissues was also an independent risk factor for metastasis (hazard ratio, 1.533; confidence interval, 1.094-2.150; P=0.013; Table II) of HBV-associated HCC. Histological grade of HCC tissues was based on the Edmondson-Steiner criteria (37). The ISHAK score of patients with HBV-associated HCC was based on the ISHAK scoring system (38).

HBx upregulates TXNIP expression in HepG2 cells. Previous studies have demonstrated that HBx may upregulate intracellular ROS levels (21), and TXNIP expression may be induced

Table I. Results of χ^2 tests to investigate the association between thioredoxin interacting protein expression level and clinicopathological features of patients with hepatitis B virus-associated hepatocellular carcinoma.

Characteristics	Low expression, n	High expression, n	χ^2 value	P-value
Age, years				
<50/≥50	18/15	17/12	0.104	0.747
Sex				
Female/male	3/30	5/24	0.912	0.339
AFP (ng/ml)				
<8/≥8	7/25	10/16	1.905	0.168
ALT (IU/l)				
<55/≥55	19/13	20/8	0.954	0.329
AST (IU/l)				
<46/≥46	14/18	18/10	2.53	0.112
HBsAg (S/CO)				
<3000/>3000	11/22	7/22	0.633	0.426
HBeAg (S/CO)				
<1/≥1	26/7	22/7	0.076	0.783
ISHAK score				
<4/≥4	6/27	7/22	0.33	0.565
Tumor size, cm				
<5/≥5	11/22	8/21	0.24	0.624
Capsule invasion				
No/yes	16/17	8/21	2.841	0.092
Histological grade				
Moderate/high	23/10	16/13	1.395	0.237
Metastasis				
No/yes	26/7	15/14	5.047	0.025

P-values were calculated using the χ^2 test. AFP, α-fetoprotein; ALT, alanine transaminase; AST, aspartate transaminase; HBsAg, surface antigen of hepatitis B virus; HBeAg, hepatitis B viral protein.

by ROS stimulation (39). However, to the best of our knowledge, no previous studies have investigated the association between HBx and TXNIP expression in HBV-associated HCC tissues or HCC cells. To investigate their clinicopathological implication and association, TXNIP and HBx mRNA levels were first investigated in HBV-associated HCC tissues. The results revealed that the mRNA levels of HBx and TXNIP were positively correlated (r=0.42; P=0.0007; Fig. 2A). The association between HBx and TXNIP was then investigated by constructing a HBx expression stable cell line with HBx expression induced and controlled by Dox. The results revealed that HBx expression was increased as Dox concentration increased (Fig. 2B), and the expression of TXNIP was upregulated as HBx expression increased (Fig. 2C). These results indicated that HBx may upregulate TXNIP expression in HepG2 cells.

The function of TXNIP in HepG2 cell migration and invasion. In the present study, high TXNIP expression was demonstrated to be positively associated with metastasis of HBV-associated HCC. The function of TXNIP in HCC cell migration and invasion was investigated by scratch migration assays and Matrigel invasion assays. The impact of TXNIP overexpression or knockdown on HepG2 cell migration and invasion were studied. Firstly, the results of western blot analysis revealed that TXNIP-EGFP fusion protein was efficiently expressed and that TXNIP expression was effectively silenced by TXNIP shRNA in HepG2 cells (Fig. 3A). The results of scratch and Matrigel assays demonstrated that TXNIP-EGFP expression may lead to increased migration (P=0.02) and invasion (P=0.004) in HepG2 cells compared with the control, while knockdown of TXNIP expression did not significantly suppress migration (P<0.05) but did significantly suppress invasion (P=0.012) of HepG2 cells (Fig. 3B and C, respectively). Therefore, TXNIP overexpression may facilitate the promotion of migration and invasion of HepG2 cells.

HBx promotes the migration and invasion of HepG2 cells through upregulating TXNIP expression. The aforementioned results indicated that HBx may upregulate TXNIP expression in HepG2 cells, and that TXNIP may have a reinforcing effect on migration and invasion of HepG2 cells. To investigate the function of TXNIP in HBx-induced migration and invasion of HCC cells, HBx was ectopically expressed with or without knockdown of TXNIP in HepG2 cells, and

Table II. Univariate and multivariate logistics regression analysis of risk factors associated with metastasis of patients with hepatitis B virus-associated hepatocellular carcinoma.

	Univariate analysis		Multivariate analysis	
Variable	HR (95% CI)	P-value	HR (95% CI)	P-value
Age, years				
<50 vs. ≥50	0.184 (0.053-0.644)	0.008	0.044 (0.004-0.443)	0.008
Gender				
Female vs. male	0.972 (0.217-4.348)	0.971		
AFP (ng/ml)				
<8 vs. ≥8	2.692 (0.664-10.913)	0.165		
ALT (IU/l)				
<55 vs. ≥55	1.385 (0.455-4.213)	0.566		
AST (IU/l)				
<46 vs. ≥46	1.654 (0.561-4.875)	0.362		
HBsAg (S/CO)				
<3000 vs. ≥3000	1.486 (0.447-4.935)	0.518		
HBeAg (S/CO)				
<1 vs. ≥1	0.729 (0.198-2.681)	0.635		
ISHAK score				
<4 vs. ≥4	0.515 (0.148-1.793)	0.297		
Tumor size, cm				
<5 vs. ≥5	6.729 (1.381-32.8)	0.018	22.25 (2.002-247.259)	0.012
Capsule invasion				
No vs. yes	6.3 (1.606-24.72)	0.008	6.561 (0.877-49.081)	0.067
Histological grade				
Moderate vs. high	5.037 (1.622-15.642)	0.005	12.185 (1.877-79.09)	0.009
TXNIP expression				
Low vs. high	1.241 (1.021-1.508)	0.03	1.533 (1.094-2.15)	0.013

HR, hazard ratio; CI, confidence interval; AFP, α-fetoprotein; ALT, alanine transaminase; AST, aspartate transaminase; HBsAg, surface antigen of hepatitis B virus; HBeAg, hepatitis B viral protein; TXNIP, thioredoxin interacting protein.

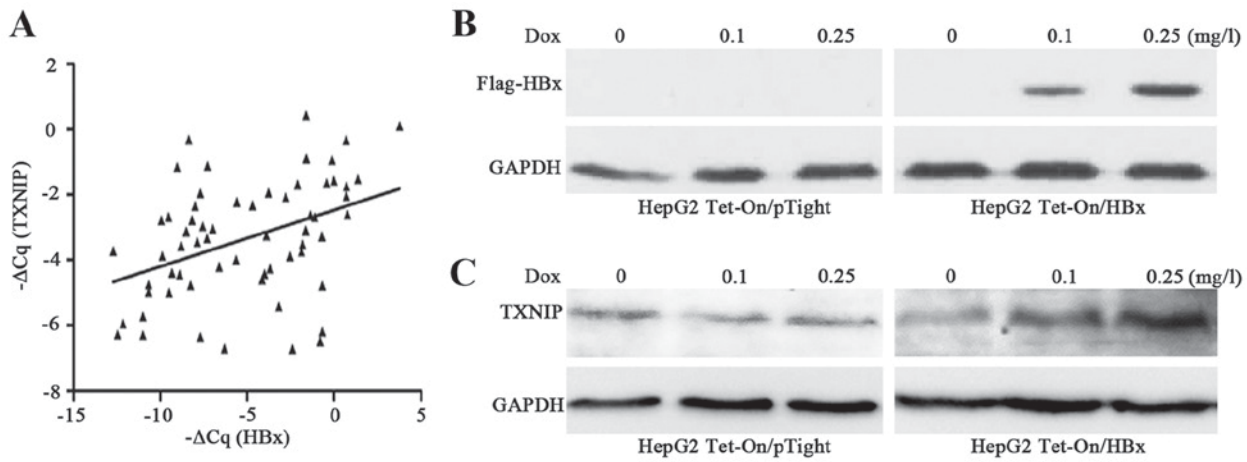

Figure 2. Correlation between TXNIP and HBx in HBV-associated hepatocellular carcinoma tissues, and HBx expression stable cell line. (A) TXNIP and HBx mRNA levels in 62 HBV-associated HCC tissues were measured by reverse transcription-quantitative polymerase chain reaction, and the -ΔCq values were assessed by Spearman correlation analysis. GAPDH was used as internal reference. HepG2 Tet-On/HBx and HepG2 Tet-On/pTight cells were then treated with the indicated concentration of Dox for 48 h, and (B) Flag-HBx and (C) TXNIP were detected by western blot analysis. GAPDH was used as input control. TXNIP, thioredoxin interacting protein; HBx hepatitis B virus X protein; HBV, hepatitis B virus; HCC, hepatocellular carcinoma; GAPDH, glyceraldehyde 3-phosphate deyhydrogenase; Dox, doxycycline.

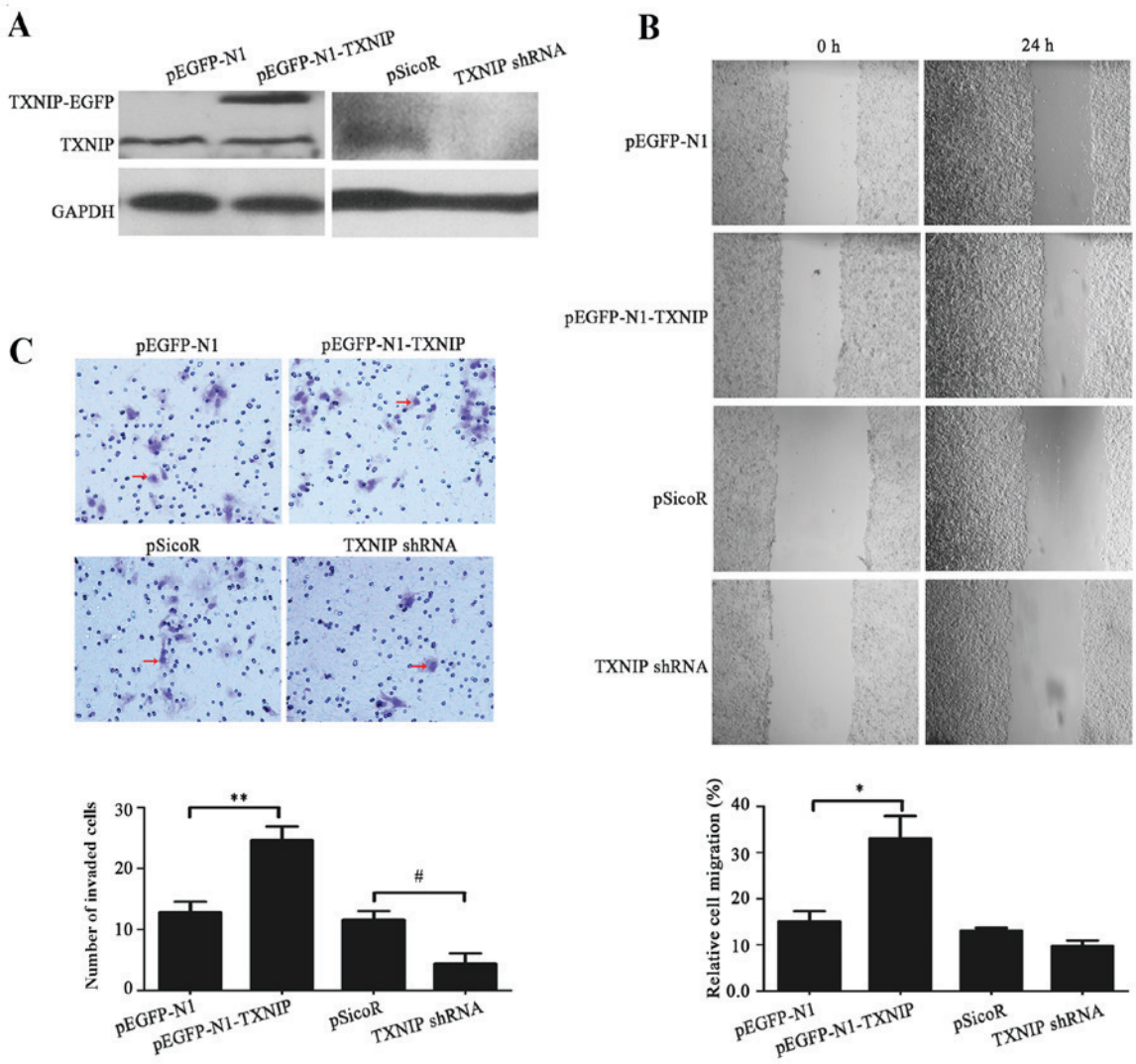

Figure 3. Effects of TXNIP overexpression on HepG2 cell migration and invasion. (A) Left: HepG2 cells were transiently transfected with pEGFP-N1-TXNIP or pEGFP-N1 TXNIP, and fusion protein TXNIP-EGFP was detected by western blot analysis. Right: HepG2 cells were infected with TXNIP shRNA lentivirus or pSicoR lentivirus. The knockdown effect on TXNIP was evaluated 72 h post-infection by western blot analysis. (B) Representative images and statistical analysis of scratch assay and (C) Matrigel invasion assay. HepG2 cells were pretreated as described in (A). Scratch migration and Matrigel invasion assays were used to evaluate the effects of TXNIP overexpression or knockdown on HepG2 cell migration and invasion, respectively. *P<0.05 and **P<0.01 vs. pEGFP-N1, $^{\#}$P<0.05 vs. pSicoR. TXNIP, thioredoxin interacting protein; EGFP, enhanced green fluorescent protein; shRNA, short hairpin RNA; GAPDH, glyceraldehyde 3-phosphate deyhydrogenase.

scratch and Matrigel assays were performed. The results of western blot analysis revealed that expression of HBx may upregulate TXNIP in HepG2 cells, while knockdown of TXNIP expression may attenuate this effect (Fig. 4A). The results of scratch and Matrigel assays revealed that HBx may promote migration (P=0.003) and invasion (P<0.001) of HepG2, respectively, while knockdown of TXNIP expression significantly attenuated HBx-mediated enhancement of migratory (P=0.003) and invasive (P<0.001) potential of HepG2 cells (Fig. 4B and C, respectively). These data indicated that HBx, potentially through upregulation of TXNIP expression, may promote the migration and invasion of HepG2 cells.

Discussion

HBx is involved in metastasis of HBV-associated HCC by various means, including upregulating intracellular ROS levels (23,24). Acting as a key mediatory factor of intracellular ROS level, TXNIP is involved in the progression of numerous types of tumor (26). However, the involvement of TXNIP in the development of HBV-associated HCC remains unclear.

TXNIP was proposed as a tumor suppressor gene in various tumors (40), including HCC (41), but its function in metastasis remains controversial. TXNIP expression levels in tumor cells of hypoxic perinecrotic areas of glioblastoma and conventional RCC are increased compared with non-hypoxic tumor cells or peritumoral tissues (42), while hypoxia often promotes cancer metastasis and leads to a poor prognosis (43,44). In an *in vitro* intravasation model study, overexpression of TXNIP in melanoma cells increased trans-endothelial intravasation compared with the control (26), while overexpression of TXNIP was reported to inhibit metastasis through the gene KiSS-1 metastasis-suppressor in melanoma cells (27). In the present study, TXNIP was detected in HBV-associated HCC tissues. TXNIP expression levels in HBV-associated

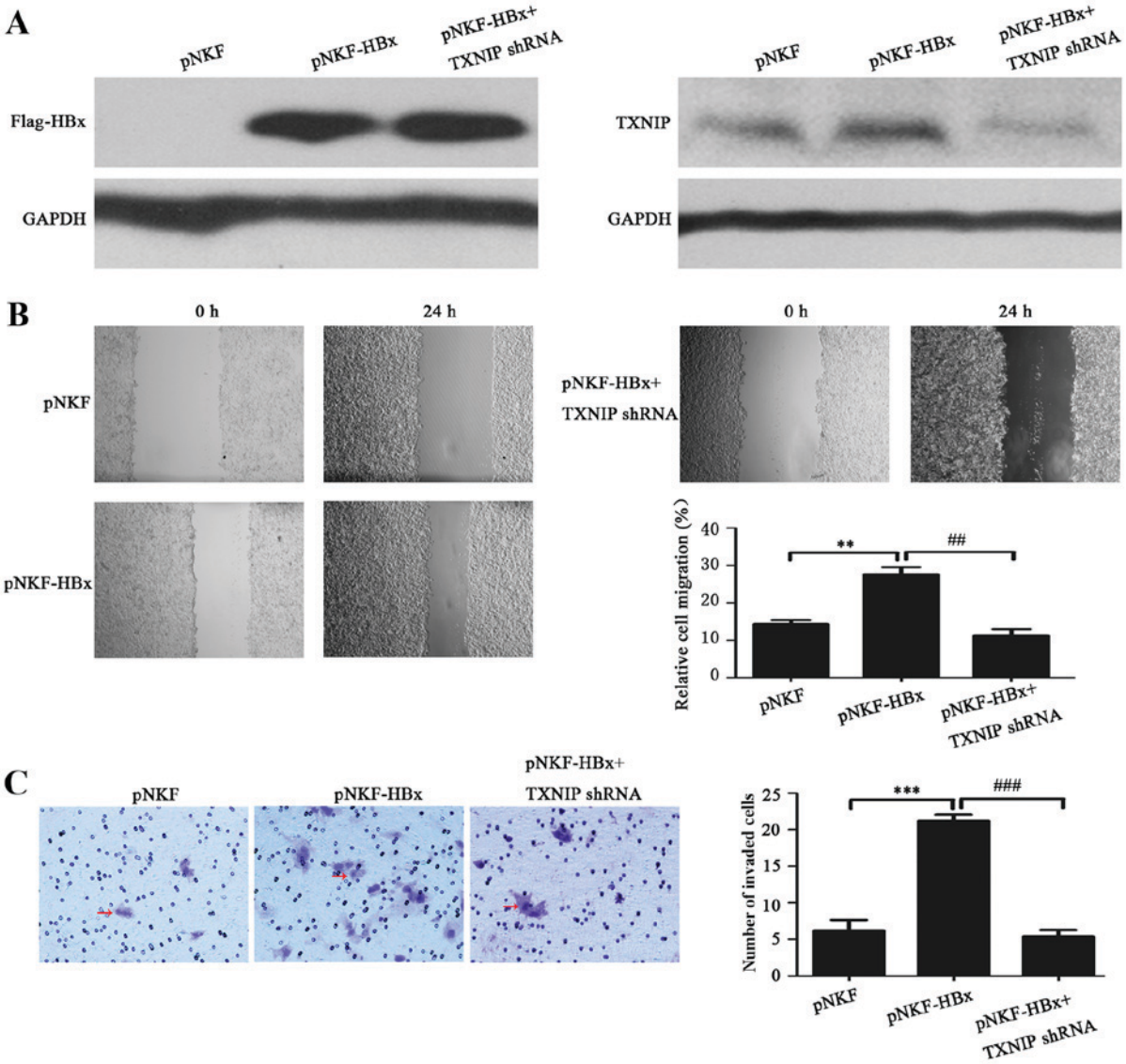

Figure 4. Function of TXNIP in HBx-induced enhancement of migration and invasion in HepG2 cells. (A) HepG2 cells were transfected with pNKF, pNKF-HBx, or infected with TXNIP shRNA lentivirus and transfected with pNKF-HBx 24 h following this. Flag-HBx and TXNIP expression was then detected by western blot analysis. (B) Representative images and statistical analysis of scratch assay and (C) Matrigel invasion assay. HepG2 cells were pretreated as described in (A). Scratch and Matrigel invasion assays were used to study the effects of ectopic expression of HBx on migratory and invasive potential of HepG2 cells and the role of TXNIP in the process. **P<0.01 and ***P<0.001 vs. pNKF; $^{\#\#}$P<0.01 and $^{\#\#\#}$P<0.001 vs. pNKF-HBx. TXNIP, thioredoxin interacting protein; HBx, hepatitis B virus X protein; shRNA, short hairpin RNA; GAPDH, glyceraldehyde 3-phosphate deyhydrogenase.

HCC tissues were revealed to be positively associated with tumor metastasis, and high expression levels of TXNIP may be an independent risk factor of metastasis. The involvement of TXNIP in regulating HCC cell migration and invasion was then studied by scratch migration assays and Matrigel invasion assays. The results demonstrated that TXNIP may enhance HepG2 cell migration and invasion. Consistent with the present findings, a previous study has demonstrated that TXNIP overexpression may increase motility and invasion of HCC cells, and may give a selective advantage to HCC cells (45). Similarly, a study on gene expression profiles of three HCC lines with different organ-tropism (accession no. GSE38945) indicated that TXNIP expression in HCC cell lines with metastasis ability to the lung and celiac lymph node is increased compared with HCC cell lines with only metastatic ability to the lung or low metastatic ability (46). The aforementioned results indicated that TXNIP may perform different functions in the occurrence and development of HBV-associated HCC. However, additional studies and more substantial investigations are required to study the involvement of TXNIP in HBV-associated HCC.

HBx was reported to increase intracellular ROS level by targeting the peroxisome or mitochondria (21,22). TXNIP was reported to be induced by stress stimulation, including infection, H_2O_2, ultraviolet and ROS (39,47). It is therefore a reasonable hypothesis that HBx may impact TXNIP expression in HBV-associated HCC tissues and HCC cells. To confirm this hypothesis, HBx and TXNIP mRNA was detected in HBV-associated HCC tissues. The results revealed that mRNA levels of HBx and TXNIP in HBV-associated HCC tissues were positively associated.

Previous studies have demonstrated that the function of HBx is associated with its expression level and subcellular distribution (48,49). Expression levels of HBx were difficult to control

by transient transfection due to different experimental conditions, promoters and cell types. Therefore, a HBx expression stable cell line was constructed based on the Tet-On Advanced inducible system for additional investigation of the association between TXNIP and HBx. The results revealed that HBx may increase TXNIP expression levels in a gradient-dependent manner in HepG2 cells. These data supported the hypothesis that HBx may impact TXNIP expression in HBV-associated HCC tissues and HCC cells.

Previous studies have indicated that ROS induced TXNIP may impair the ability of cells to remove intracellular ROS (23,50,51), while increased intracellular ROS may contribute to the metastatic process of HBV-associated HCC (23,24,52). Whether TXNIP is involved in HBx-induced metastasis of HBV-associated HCC is worthy of further study. Scratch and Matrigel assays were employed to study the involvement of TXNIP in HBx regulation of HCC cell migration and invasion. Results revealed that HBx expression in HepG2 cells markedly enhanced cell migration and invasion ability, which is consistent with the results of previous studies (18,53). The increase of cell migration and invasion was attenuated by knockdown of TXNIP expression. These data indicated that HBx, is involved in promoting migration and invasion of HCC cells, potentially through upregulating TXNIP expression.

As a non-structural protein, HBx has a short half-life of only ~30 min; and its concentration in cells or tissues is too low to detect (54,55). Previous studies have indicated that HBx is degraded in a ubiquitin-proteasome pathway (56,57). In addition, previous studies have demonstrated that HBx may be highly expressed in HepG2 cells transiently transfected with HBx expression plasmids, but its expression in the HBx expression stable cell line is weak (54,58). In the present study, HBx expression stable cell lines were treated with proteasome inhibitors MG132 prior to western blot analysis.

In summary, to the best of our knowledge, the present study was the first to identify that high expression of TXNIP in HBV-associated HCC tissues may be an independent risk factor for metastasis. Utilizing scratch migration assays and Matrigel invasion assays, it was confirmed that overexpression of TXNIP in HepG2 cells enhanced cell migration and invasion, and TXNIP may be involved in HBx-induced enhancement of cell migration and invasion. Additional investigations designed to study the mechanisms of HBx-induced upregulation of TXNIP and TXNIP-induced migration and invasion of HepG2 cells are required.

Acknowledgements

The present study was supported by research grants from the National Basic Research Program of China (grant no. 2013CB911300) and the National Natural Science Foundation of China (grant no. 81371796).

References

1. El-Serag HB and Rudolph KL: Hepatocellular carcinoma: Epidemiology and molecular carcinogenesis. Gastroenterology 132: 2557-2576, 2007.
2. Shlomai A, de Jong YP and Rice CM: Virus associated malignancies: The role of viral hepatitis in hepatocellular carcinoma. Semin Cancer Biol 26: 78-88, 2014.
3. Weinmann A, Koch S, Niederle IM, Schulze-Bergkamen H, König J, Hoppe-Lotichius M, Hansen T, Pitton MB, Düber C, Otto G, *et al*: Trends in epidemiology, treatment, and survival of hepatocellular carcinoma patients between 1998 and 2009: An analysis of 1066 cases of a German HCC Registry. J Clin Gastroenterol 48: 279-289, 2014.
4. Paranagua-Vezozzo DC, Ono SK, Alvarado-Mora MV, Farias AQ, Cunha-Silva M, França JI, Alves VA, Sherman M and Carrilho FJ: Epidemiology of HCC in Brazil: Incidence and risk factors in a ten-year cohort. Annals of hepatology 13: 386-393, 2014.
5. Ye QH, Qin LX, Forgues M, He P, Kim JW, Peng AC, Simon R, Li Y, Robles AI, Chen Y, *et al*: Predicting hepatitis B virus-positive metastatic hepatocellular carcinomas using gene expression profiling and supervised machine learning. Nat Med 9: 416-423, 2003.
6. Tang H, Delgermaa L, Huang F, Oishi N, Liu L, He F, Zhao L and Murakami S: The transcriptional transactivation function of HBx protein is important for its augmentation role in hepatitis B virus replication. J Virol 79: 5548-5556, 2005.
7. Tang H, Oishi N, Kaneko S and Murakami S: Molecular functions and biological roles of hepatitis B virus x protein. Cancer Sci 97: 977-983, 2006.
8. Tarocchi M, Polvani S, Marroncini G and Galli A: Molecular mechanism of hepatitis B virus-induced hepatocarcinogenesis. World J Gastroenterol 20: 11630-11640, 2014.
9. Buendia MA and Neuveut C: Hepatocellular carcinoma. Cold Spring Harb Perspect Med 5: a021444, 2015.
10. Bharadwaj M, Roy G, Dutta K, Misbah M, Husain M and Hussain S: Tackling hepatitis B virus-associated hepatocellular carcinoma-the future is now. Cancer Metastasis Rev 32: 229-268, 2013.
11. Tian Y, Yang W, Song J, Wu Y and Ni B: Hepatitis B virus X protein-induced aberrant epigenetic modifications contributing to human hepatocellular carcinoma pathogenesis. Mol Cell Biol 33: 2810-2816, 2013.
12. Yang SZ, Zhang AQ, Chen G, Zhang LD, Zhu J, Li XW and Dong JH: Experimental study of epithelial-mesenchymal transition induced by HBx protein in liver cancer cell. Zhonghua Yi Xue Za Zhi 90: 818-821, 2010.
13. Teng J, Wang X, Xu Z and Tang N: HBx-dependent activation of Twist mediates STAT3 control of epithelium-mesenchymal transition of liver cells. J Cell Biochem 114: 1097-1104, 2013.
14. Lara-Pezzi E, Gómez-Gaviro MV, Gálvez BG, Mira E, Iñiguez MA, Fresno M, Martínez-A C, Arroyo AG and López-Cabrera M: The hepatitis B virus X protein promotes tumor cell invasion by inducing membrane-type matrix metalloproteinase-1 and cyclooxygenase-2 expression. J Clin Invest 110: 1831-1838, 2002.
15. Ou DP, Tao YM, Tang FQ and Yang LY: The hepatitis B virus X protein promotes hepatocellular carcinoma metastasis by upregulation of matrix metalloproteinases. Int J Cancer 120: 1208-1214, 2007.
16. Lara-Pezzi E, Majano PL, Yáñez-Mó M, Carretero M, Moreno-Otero R, Sánchez-Madrid F and López-Cabrera M: Effect of the hepatitis B virus HBx protein on integrin-mediated adhesion to and migration on extracellular matrix. J Hepatol 34: 409-415, 2001.
17. Lara-Pezzi E, Serrador JM, Montoya MC, Zamora D, Yáñez-Mó M, Carretero M, Furthmayr H, Sánchez-Madrid F and López-Cabrera M: The hepatitis B virus X protein (HBx) induces a migratory phenotype in a CD44-dependent manner: Possible role of HBx in invasion and metastasis. Hepatology 33: 1270-1281, 2001.
18. Huang JF, Guo YJ, Zhao CX, Yuan SX, Wang Y, Tang GN, Zhou WP and Sun SH: Hepatitis B virus X protein (HBx)-related long noncoding RNA (lncRNA) down-regulated expression by HBx (Dreh) inhibits hepatocellular carcinoma metastasis by targeting the intermediate filament protein vimentin. Hepatology 57: 1882-1892, 2013.
19. Xu X, Fan Z, Kang L, Han J, Jiang C, Zheng X, Zhu Z, Jiao H, Lin J, Jiang K, *et al*: Hepatitis B virus X protein represses miRNA-148a to enhance tumorigenesis. J Clin Invest 123: 630-645, 2013.
20. Zhang X, Liu S, Hu T, Liu S, He Y and Sun S: Up-regulated microRNA-143 transcribed by nuclear factor kappa B enhances hepatocarcinoma metastasis by repressing fibronectin expression. Hepatology 50: 490-499, 2009.
21. Zou LY, Zheng BY, Fang XF, Li D, Huang YH, Chen ZX, Zhou LY and Wang XZ: HBx co-localizes with COXIII in HL-7702 cells to upregulate mitochondrial function and ROS generation. Oncol Rep 33: 2461-2467, 2015.

22. Waris G, Huh KW and Siddiqui A: Mitochondrially associated hepatitis B virus X protein constitutively activates transcription factors STAT-3 and NF-kappa B via oxidative stress. Mol Cell Biol 21: 7721-7730, 2001.
23. Li W, Wu Z, Ma Q, Liu J, Xu Q, Han L, Duan W, Lv Y, Wang F, Reindl KM and Wu E: Hyperglycemia regulates TXNIP/TRX/ROS axis via p38 MAPK and ERK pathways in pancreatic cancer. Curr Cancer Drug Targets 14: 348-356, 2014.
24. Wu WS: The signaling mechanism of ROS in tumor progression. Cancer Metastasis Rev 25: 695-705, 2006.
25. Yoshihara E, Masaki S, Matsuo Y, Chen Z, Tian H and Yodoi J: Thioredoxin/Txnip: Redoxisome, as a redox switch for the pathogenesis of diseases. Front Immunol 4: 514, 2014.
26. Cheng GC, Schulze PC, Lee RT, Sylvan J, Zetter BR and Huang H: Oxidative stress and thioredoxin-interacting protein promote intravasation of melanoma cells. Exp Cell Res 300: 297-307, 2004.
27. Goldberg SF, Miele ME, Hatta N, Takata M, Paquette-Straub C, Freedman LP and Welch DR: Melanoma metastasis suppression by chromosome 6: Evidence for a pathway regulated by CRSP3 and TXNIP. Cancer Res 63: 432-440, 2003.
28. Masaki S, Masutani H, Yoshihara E and Yodoi J: Deficiency of thioredoxin binding protein-2 (TBP-2) enhances TGF-b signaling and promotes epithelial to mesenchymal transition. PloS One 7: e39900, 2012.
29. Wei J, Shi Y, Hou Y, Ren Y, Du C, Zhang L, Li Y and Duan H: Knockdown of thioredoxin-interacting protein ameliorates high glucose-induced epithelial to mesenchymal transition in renal tubular epithelial cells. Cell Signal 25: 2788-2796, 2013.
30. Wu DB, Liu FW, Li J, Liu C, Liu L, Chen EQ, Zhao LS, Tang H and Zhou TY: Intrahepatic IFN-alpha expression in liver specimens from HBV-infected patients with different outcomes. Eur Rev Med Pharmacol Sci 17: 2474-2480, 2013.
31. Xia L, Huang W, Tian D, Zhang L, Qi X, Chen Z, Shang X, Nie Y and Wu K: Forkhead box Q1 promotes hepatocellular carcinoma metastasis by transactivating ZEB2 and VersicanV1 expression. Hepatology 59: 958-973, 2014.
32. Chen W, Li M, Su GZ, Cao J, Sang W, Zhao K, Wu QY, Zhu F and Xu KL: Establishment of mouse mesenchymal stem cells overexpressing CXCR4 gene and evaluation of their functions. Zhongguo Shi Yan Xue Ye Xue Za Zhi 22: 1391-1395, 2014.
33. Livak KJ and Schmittgen TD: Analysis of relative gene expression data using real-time quantitative PCR and the 2(-Delta Delta C (T)) Method. Methods 25: 402-408, 2001.
34. Bai L, Xu X, Wang Q, Xu S, Ju W, Wang X, Chen W, He W, Tang H and Lin Y: A superoxide-mediated mitogen-activated protein kinase phosphatase-1 degradation and c-Jun NH(2)-terminal kinase activation pathway for luteolin-induced lung cancer cytotoxicity. Mol Pharmacol 81: 549-555, 2012.
35. Dasari VR, Kaur K, Velpula KK, Gujrati M, Fassett D, Klopfenstein JD, Dinh DH and Rao JS: Upregulation of PTEN in glioma cells by cord blood mesenchymal stem cells inhibits migration via downregulation of the PI3K/Akt pathway. PloS One 5: e10350, 2010.
36. Shi R, Zhao Z, Zhou H, Wei M, Ma WL, Zhou JY and Tan WL: Reduced expression of PinX1 correlates to progressive features in patients with prostate cancer. Cancer Cell Int 14: 46, 2014.
37. Edmondson HA and Steiner PE: Primary carcinoma of the liver: A study of 100 cases among 48,900 necropsies. Cancer 7: 462-503, 1954.
38. Ishak K, Baptista A, Bianchi L, Callea F, De Groote J, Gudat F, Denk H, Desmet V, Korb G, MacSween RN, *et al*: Histological grading and staging of chronic hepatitis. J Hepatol 22: 696-699, 1995.
39. Zhang X, Zhang JH, Chen XY, Hu QH, Wang MX, Jin R, Zhang QY, Wang W, Wang R, Kang LL, *et al*: Reactive oxygen species-induced TXNIP drives fructose-mediated hepatic inflammation and lipid accumulation through NLRP3 inflammasome activation. Antioxid Redox Signal 22: 848-870, 2015.
40. Zhou J, Yu Q and Chng WJ: TXNIP (VDUP-1, TBP-2): A major redox regulator commonly suppressed in cancer by epigenetic mechanisms. Int J Biochem Cell Biol 43: 1668-1673, 2011.
41. Sheth SS, Bodnar JS, Ghazalpour A, Thipphavong CK, Tsutsumi S, Tward AD, Demant P, Kodama T, Aburatani H and Lusis AJ: Hepatocellular carcinoma in Txnip-deficient mice. Oncogene 25: 3528-3536, 2006.
42. Le Jan S, Le Meur N, Cazes A, Philippe J, Le Cunff M, Léger J, Corvol P and Germain S: Characterization of the expression of the hypoxia-induced genes neuritin, TXNIP and IGFBP3 in cancer. FEBS Lett 580: 3395-3400, 2006.
43. Semenza GL: The hypoxic tumor microenvironment: A driving force for breast cancer progression. Biochim Biophys Acta 1863: 382-391, 2016.
44. Fraga A, Ribeiro R, Príncipe P, Lopes C and Medeiros R: Hypoxia and prostate cancer aggressiveness: A tale with many endings. Clin Genitourin Cancer 13: 295-301, 2015.
45. Gunes A, Iscan E, Topel H, Avci ST, Gumustekin M, Erdal E and Atabey N: Heparin treatment increases thioredoxin interacting protein expression in hepatocellular carcinoma cells. Int J Biochem Cell Biol 65: 169-181, 2015.
46. Tao ZH, Wu WZ, Wang XL, Wan JL, Sun HC, Wang L, Xia JL and Fan J: The establishment of a systematic site-specific metastasis model of human hepatocellular carcinoma in nude mouse. Zhonghua Gan Zang Bing Za Zhi 19: 110-113, 2011.
47. Junn E, Han SH, Im JY, Yang Y, Cho EW, Um HD, Kim DK, Lee KW, Han PL, Rhee SG and Choi I: Vitamin D3 up-regulated protein 1 mediates oxidative stress via suppressing the thioredoxin function. J Immunol 164: 6287-6295, 2000.
48. Ma J, Sun T, Park S, Shen G and Liu J: The role of hepatitis B virus X protein is related to its differential intracellular localization. Acta Biochim Biophys Sin (Shanghai) 43: 583-588, 2011.
49. Henkler F, Hoare J, Waseem N, Goldin RD, McGarvey MJ, Koshy R and King IA: Intracellular localization of the hepatitis B virus HBx protein. J Gen Virol 82: 871-882, 2001.
50. Singh LP: Thioredoxin interacting protein (TXNIP) and pathogenesis of diabetic retinopathy. J Clin Exp Ophthalmol 4: 2013.
51. Li X, Rong Y, Zhang M, Wang XL, LeMaire SA, Coselli JS, Zhang Y and Shen YH: Up-regulation of thioredoxin interacting protein (Txnip) by p38 MAPK and FOXO1 contributes to the impaired thioredoxin activity and increased ROS in glucose-treated endothelial cells. Biochem Biophys Res Commun 381: 660-665, 2009.
52. Han JM, Kang JA, Han MH, Chung KH, Lee CR, Song WK, Jun Y and Park SG: Peroxisome-localized hepatitis Bx protein increases the invasion property of hepatocellular carcinoma cells. Arch Virol 159: 2549-2557, 2014.
53. Ryu SH, Jang MK, Kim WJ, Lee D and Chung YH: Metastatic tumor antigen in hepatocellular carcinoma: Golden roads toward personalized medicine. Cancer Metastasis Rev 33: 965-980, 2014.
54. Schek N, Bartenschlager R, Kuhn C and Schaller H: Phosphorylation and rapid turnover of hepatitis B virus X-protein expressed in HepG2 cells from a recombinant vaccinia virus. Oncogene 6: 1735-1744, 1991.
55. Kim JH, Kang S, Kim J and Ahn BY: Hepatitis B virus core protein stimulates the proteasome-mediated degradation of viral X protein. J Virol 77: 7166-7173, 2003.
56. Zhang Z, Sun E, Ou JH and Liang TJ: Inhibition of cellular proteasome activities mediates HBX-independent hepatitis B virus replication in vivo. J Virol 84: 9326-9331, 2010.
57. Hu Z, Zhang Z, Doo E, Coux O, Goldberg AL and Liang TJ: Hepatitis B virus X protein is both a substrate and a potential inhibitor of the proteasome complex. J Virol 73: 7231-7240, 1999.
58. McClain SL, Clippinger AJ, Lizzano R and Bouchard MJ: Hepatitis B virus replication is associated with an HBx-dependent mitochondrion-regulated increase in cytosolic calcium levels. J Virol 81: 12061-12065, 2007.